Separation Science and Technology
Publication details, including instructions for authors and subscription information:
http://www.informaworld.com/smpp/title~content=t713708471

Hydroxyapatite High-Performance Liquid Chromatography: Detailed Investigations on Chromatographic Efficiencies for the Case of Plate-Like Crystals

Tsutomu Kawasaki[a]; Shoichi Takahashi[a]
[a] CHROMATOGRAPHIC RESEARCH LABORATORY KOKEN CO. LTD., TOKYO, JAPAN

To cite this Article Kawasaki, Tsutomu and Takahashi, Shoichi(1988) 'Hydroxyapatite High-Performance Liquid Chromatography: Detailed Investigations on Chromatographic Efficiencies for the Case of Plate-Like Crystals', Separation Science and Technology, 23: 1, 193 — 214
To link to this Article: DOI: 10.1080/01496398808057642
URL: http://dx.doi.org/10.1080/01496398808057642

SEPARATION SCIENCE AND TECHNOLOGY, 23(1-3), pp. 193-214, 1988

Hydroxyapatite High-Performance Liquid Chromatography: Detailed Investigations on Chromatographic Efficiencies for the Case of Plate-Like Crystals

TSUTOMU KAWASAKI and SHOICHI TAKAHASHI

CHROMATOGRAPHIC RESEARCH LABORATORY
KOKEN CO. LTD.
3-5-18 SHIMO-OCHIAI, SHINJUKU-KU, TOKYO 161, JAPAN

Abstract

Earlier, hydroxyapatite (HA) high-performance liquid chromatography (HPLC) using plate-like crystals was developed. With this HPLC, behaviors of both elution molarity and standard deviation of chromatographic peak are investigated as functions of (a) sample load, (b) flow rate, (c) total column length, and (d) slope of the molarity gradient of the development buffer; from these data, experimental conditions giving optimal chromatographic efficiencies are explored. On the basis of the present study, previously obtained HPLC data are reconsidered. The present study is compared with the earlier study of classical open HA columns. Finally, the data are analyzed on the basis of the chromatographic theory developed earlier, from which important information is available.

Abbreviations. ϕ, inside column diameter. Buffer A, potassium phosphate buffer at pH $\approx$ 6.8. P, pressure drop. T, temperature.

INTRODUCTION

Three types of hydroxyapatite (HA) high-performance liquid chromatography (HPLC) have been developed in our laboratory. These involve using columns packed with plate-like HA crystals with thicknesses of about 1–3 μm and diameters of several times 10 μm (*1*, *2*); using columns packed with spherical aggregates with diameters of 1–10 μm of HA

microcrystals (*3*, *4*); and using columns packed with square tile-shaped HA crystals with thicknesses of about 2 μm and diameters of 3–7 μm (*5*).

The present paper is concerned with plate-like HA packed columns; these are characterized by a low pressure drop and a very high overall column length available by connecting columns in series using fine tubes (*1*, *2*). The purpse of this paper is to investigate for the case of the gradient elution mode, the behaviors of both elution molarity and standard deviation of chromatographic peak as functions of the following experimental parameters: (a) sample load, (b) flow rate, (c) total column length, and (d) slope of the molarity gradient of the development buffer. From these data, experimental conditions giving optimal chromatographic efficiencies are explored. Both lysozyme and DNA are used as probes. [Earlier (*6–8*), similar investigations were carried out for classical open HA columns, the T_2 phage data of which are here used as a reference.]

In the Appendix a brief summary of the general theory of quasi-static linear gradient chromatography is given; this was developed in earlier papers (*8–11*). In Discussion Subsection B, the experimental data obtained in the present paper are analyzed on the basis of the chromatographic theory.

MATERIALS AND METHODS

Both plate-like HA crystals [with thicknesses of about 1–3 μm and diameters of several times 10 μm; H-type crystals (*1*)] and HA-packed SUS316 stainless steel columns (KB columns; Koken Co. Ltd., Tokyo, Japan) were prepared in our laboratory. The inside column diameter was always 6 mm; lengths of 0.5, 1, 3, 10, and 30 cm were prepared. The 3-cm column was used as either a precolumn or a main column. If a large overall column length was necessary, it was provided by connecting 30-cm columns in series using fine tubes.

The HPLC experiments were carried out by connecting the column or column system to an HPLC pump. Material was eluted using a linear molarity gradient of potassium phosphate buffer at pH $\approx$ 6.8 (i.e., an equimolar mixture of K_2HPO_4 and KH_2PO_4; called buffer A). The sample elution was monitored by measuring the ultraviolet absorption in a flow cell. At the same time the molarity gradient was monitored by measuring the refractive index in a special flow cell with a low angle.

The ratio of the volume occupied by HA crystals to the total packed crystal volume in the column was estimated to be 0.075 by measuring the

dry weight of the packed crystals and by calculating the dry crystal volume on the basis of the crystal structure of HA (cf. Ref. *1*).

The samples applied to chromatography were limited to lysozyme (from chicken egg white, Sigma) and DNA with molecular masses of the order of 10–50 MDa from human placenta, prepared according to Ref. *12* (a gift from Dr J. Filipski of the laboratory of Prof G. Bernardi, Institut Jacques Monod, Université Paris VII, Paris, France).

IMPORTANT EXPERIMENTAL PARAMETERS

Experimental parameters which will play important roles are defined below. The parameters are limited to those that can be defined without knowledge of the chromatographic theory presented in the Appendix.

$m_{(P)}$ and $m_{(K^+)}$: phosphate and potassium molarity in buffer A, respectively. $m_{(K^+)}$ is 1.5 times as large as $m_{(P)}$.

$m_{elu(P)}$: elution phosphate molarity, i.e., the phosphate molarity in the buffer A gradient at which the maximum height of the chromatographic peak is eluted. In the case of the DNA peak having a large width because of molecular heterogeneity (cf. Fig 2 of Ref. *2*), however, m_{elu} is defined as the phosphate molarity at which the center of gravity of the peak is eluted.

$m_{elu(K^+)}$: elution potassium molarity, i.e., the potassium molarity in the buffer A gradient at which the maximum height of the chromatographic peak is eluted. $m_{elu(K^+)}$ is 1.5 times as large as $m_{elu(P)}$.

$m_{in(P)}$ and $m_{in(K^+)}$: initial phosphate and potassium molarity, i.e., the phosphate and potassium molarity in buffer A occurring before the buffer A gradient begins, respectively. $m_{in(K^+)}$ is 1.5 times as large as $m_{in(P)}$.

$\sigma_{(P)}$: standard deviation (with a dimension of m*M*) of the chromatographic peak measured in terms of the phosphate molarity range of the buffer A gradient over which the peak appears. Here, $\sigma_{(P)}$ is represented approximately as the half-width at 0.6065 times the maximum height of the peak; this is exactly equal to the standard deviation provided the peak has a precise Gaussian shape.

$\sigma_{(K^+)}$: standard deviation (with a dimension of m*M*) measured in terms of the potassium molarity range of the buffer A gradient instead of the phosphate range. $\sigma_{(K^+)}$ is 1.5 times as large as $\sigma_{(P)}$.

$g'_{(P)}$ and $g'_{(P)}(\phi = 1\ \text{cm})$: $g'_{(P)}$ represents the slope concerning the phosphate molarity gradient in the buffer A gradient, measured in unit of *M*/mL

or mM/mL. $g'_{(P)}(\phi = 1$ cm) represents the reduced $g'_{(P)}$ to inside column diameter $\phi = 1$ cm. $g'_{(P)}(\phi = 1$ cm) is 0.36 ($= 0.6^2$) time as large as $g'_{(P)}$.

$g'_{(K^+)}$ and $g'_{(K^+)}(\phi = 1$ cm): slope and reduced slope (to $\phi = 1$ cm) concerning the potassium molarity gradient in the buffer A gradient, being 1.5 times as large as $g'_{(P)}$ and $g'_{(P)}(\phi = 1$ cm), respectively. $g'_{(K^+)}(\phi = 1$ cm) is 0.36 time as large as $g'_{(K^+)}$.

L: total (overall) column length measured in centimeters.

$s_{app(P)}$ and $s_{app(K^+)}$: products of $g'_{(P)}(\phi = 1$ cm) and L, and of $g'_{(K^+)}(\phi = 1$ cm) and L, respectively.

B': partition of sample molecules in mobile phase occurring in an elementary volume of the column, or the ratio of the amount of molecules in mobile phase to the total amount in that elementary volume. B', therefore, varies between 0 and 1, increasing, in general, with an increase of $m_{(P)}$ or $m_{(K^+)}$.

RESULTS

(A) Lysozyme

Figures 1(a) and (b), respectively, represent $m_{elu(P)}$ and $\sigma_{(P)}$ for the lysozyme chromatographic peak as functions of sample load when $L = 13$ cm, $g'_{(P)} = 3.47$ mM/mL [$g'_{(P)}(\phi = 1$ cm) = 1.25 mM/mL], and flow rate = 1.5 mL/min [reduced value (to $\phi = 1$ cm) = 4.17 mL/min]. It can be seen that $m_{elu(P)}$ decreases slowly (Fig. 1a) and that $\sigma_{(P)}$ increases more rapidly (Fig. 1b) with an increase in sample load; both $m_{elu(P)}$ and $\sigma_{(P)}$ approach *finite* values when sample load tends to infinitesimal. This means that both $m_{elu(P)}$ and $\sigma_{(P)}$ are independent of sample load when sample load is small enough; this observation is widely experienced for a variety of chromatographies.

Figures 2(a) and (b), respectively, represent $m_{elu(P)}$ and $\sigma_{(P)}$ as functions of flow rate when L and $g'_{(P)}$ are equal to those used in both Figs. 1(a) and (b) and when sample load is fixed to 0.15 mg. The fact that $m_{elu(P)}$ is virtually independent of flow rate (Fig. 2a) is consistent with the first principle of chromatography (Appendix III of Ref. *11*).

It can be shown that the dependence of $m_{elu(P)}$ upon sample load and the dependences of $\sigma_{(P)}$ upon both sample load and flow rate are generally reduced if L increases and $g'_{(P)}$ decreases. It can be deduced that the sample loads applied in Figs. 3, 4(a), and 4(b) are samll enough for both m_{elu} and $\sigma_{(P)}$ to be virtually independent of sample load.

The points in Fig. 3(a) are experimental plots of $m_{elu(P)}$ or $m_{elu(K^+)}$ versus

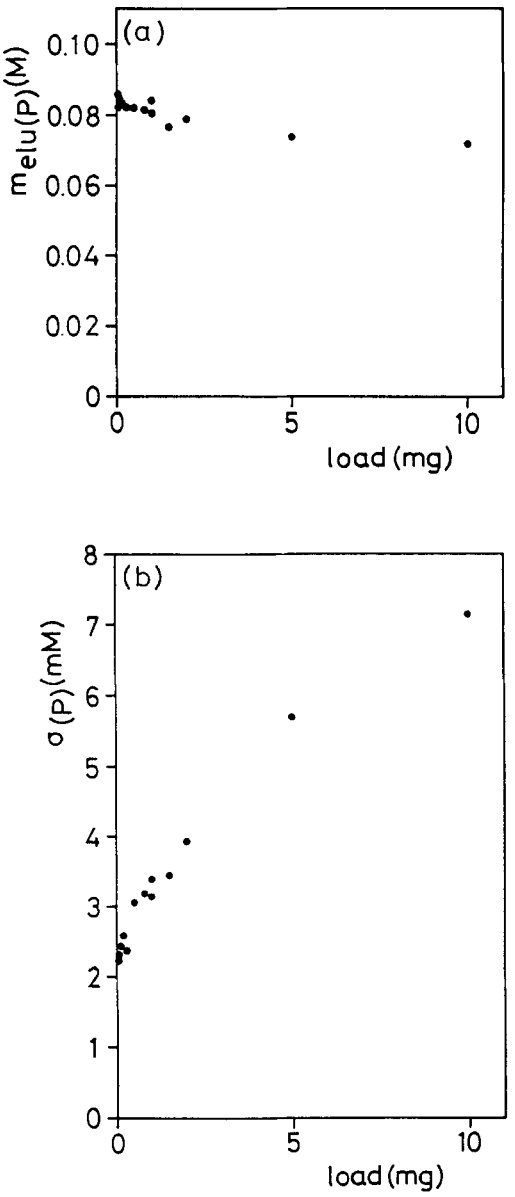

FIG. 1. (a) $m_{elu(P)}$ and (b) $\sigma_{(P)}$ for lysozyme as functions of sample load as obtained when $L = 3 + 10 = 13$ cm, $g'_{(P)} = 3.47$ mM/mL [$g'_{(P)}(\phi = 1$ cm$) = 1.25$ mM/mL], and flow rate = 1.5 mL/min [reduced value (to $\phi = 1$ cm) = 4.17 mL/min]; reduced sample load (to $\phi = 1$ cm) is 2.78 ($= 1/0.6^2$) times as large as the actual load. Other experimental conditions are: $m_{in(P)} = 1$ mM, $P = 0.7$–1.7 MPa, $T = 17.5$–20.2°C.

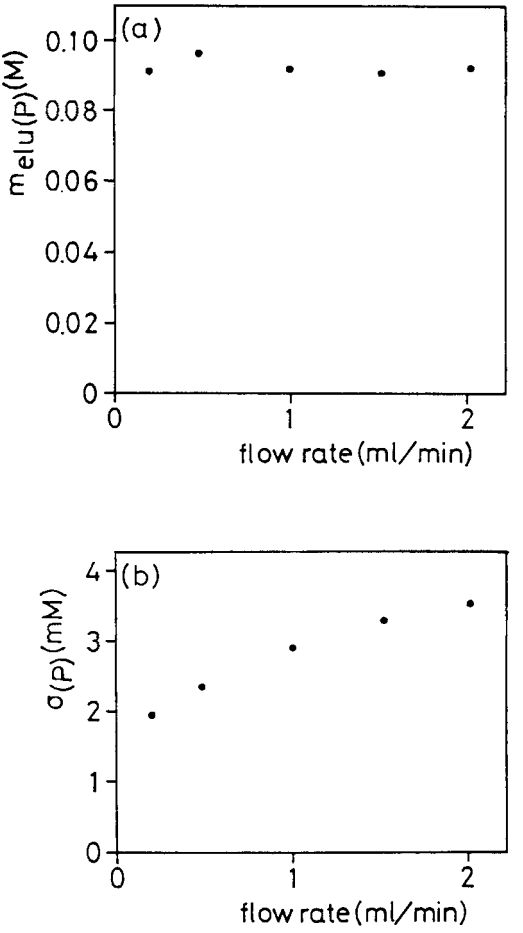

FIG. 2. (a) $m_{elu(P)}$ and (b) $\sigma_{(P)}$ for lysozyme as functions of flow rate as obtained when $L = 3 + 10 = 13$ cm, $g'_{(P)} = 3.47$ mM/mL [$g'_{(P)}(\phi = 1$ cm$) = 1.25$ mM/mL], and sample load = 0.15 mg [reduced value (to $\phi = 1$ cm) = 0.42 mg]; reduced flow rate (to $\phi = 1$ cm) is 2.78 ($= 1/0.6^2$) times as large as the actual flow rate. Other experimental conditions are: $m_{in(P)} = 1$ mM, $P = 0.1$–1.0 MPa, $T = 17.9$–19.5°C.

L for five different $g'_{(P)}$ [or $g'_{(P)}(\phi = 1$ cm$)$] values: 10.4 (or 3.75), 3.47 (or 1.25), 1.25 (or 0.45), 0.625 (or 0.225), and 0.104 (or 0.0375) mM/mL; the corresponding sample loads are 0.08, 0.15, 0.25, 0.35, and 0.85 mg, respectively. In Fig. 4(a) some experimental plots in Fig. 3(a) are picked up in order to compare the plots with those for both DNA and T_2 phage.

[Similar plots for several proteins are illustrated in the earlier paper (*6*) for classical open HA columns.] It can be seen in Fig. 3(a) that the dependence of $m_{elu(P)}$ or $m_{elu(K^+)}$ upon L differs when $g'_{(P)}$ or $g'_{(K^+)}$ applied is different, giving five arrangements of the experimental points corresponding to the five values of $g'_{(P)}$ or $g'_{(K^+)}$.

The continuous curves in both Figs. 3(a) and 4(a) are theoretical, calculated by using Eq. (5) in the Appendix (see Discussion Section B).

The points in Fig. 4(b) are experimental plots of $m_{elu(P)}$ or $m_{elu(K^+)}$ versus $\ln s_{app}$ or $\ln s_{app(K^+)}$ instead of L where the same experimental data as used in Fig. 3(a) are applied. It can be seen in Fig. 4(b) that the five arrangements of the experimental points in Fig. 3(a) converge into a single arrangement.

The continuous curve in Fig. 4(b) is theoretical, calculated by using Eq. (5) in the Appendix. (See Discussion Section B; the corresponding experimental plots and theoretical curves for classical open HA columns are illustrated in Refs. *7* and *8*.)

The points in Fig. 3(b) are experimental plots of $\sigma_{(P)}$ or $\sigma_{(K^+)}$ versus L for the five $g'_{(P)}$ values in Fig. 3(a) where the same experimental data as used in both Figs. 3(a) and 4(b) are applied. It can be seen in Fig. 3(b) that $\sigma_{(P)}$ or $\sigma_{(K^+)}$, in general, decreases very rapidly with an increase of L when L is small, but that $\sigma_{(P)}$ or $\sigma_{(K^+)}$ increases slowly after the first rapid decrease. The L value giving $\sigma_{(P)}$ or $\sigma_{(K^+)}$ the minimum value increases, and the minimum $\sigma_{(P)}$ or $\sigma_{(K^+)}$ value decreases when $g'_{(P)}$ or $g'_{(K^+)}$ decreases (Fig. 3b); when $g'_{(P)} \leqslant 1.25$ mM/mL, the slow increase of $\sigma_{(P)}$ or $\sigma_{(K^+)}$ with an increase of L can be assumed to occur outside the scope of Fig. 3(b).

The continuous and dotted curves in Fig. 3(b) are theoretical, calculated by using Eq. (6) in the Appendix. (See Discussion Subsection B; the corresponding experimental plots and theoretical curves obtained for classical open HA columns are illustrated in Ref. *8*. The experimental plots in Ref. *8* fluctuate much more than the present plots, however.)

Since the parameters q, $\varphi'_{(K^+)}$, and x' (Appendix) can be evaluated from Fig. 4(b) (cf. the legend of Fig. 4b and Discussion Subsection B), it is now possible to calculate the parameter B' for lysozyme as a function of $m_{(K^+)}$ by using Eq. (3) in the Appendix. The result of the calculation is shown in Fig. 4(g); the importance of Fig. 4(g) will be mentioned in Discussion Subsection A.

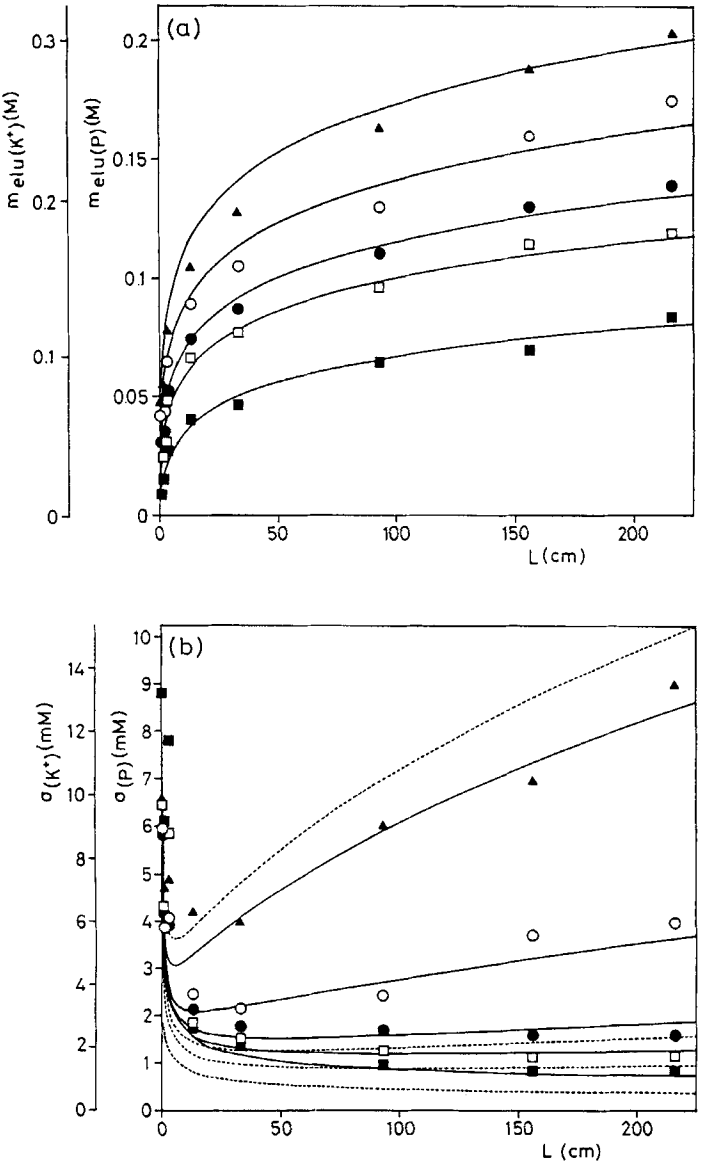

FIG. 3. Points: experimental plots of (a) $m_{elu(P)}$ or $m_{elu(K^+)}$ and (b) $\sigma_{(P)}$ or $\sigma_{(K^+)}$ for lysozyme versus L for five different $g'_{(P)}$ [or $g'_{(P)}(\phi = 1$ cm)] values: 10.4 (or 3.75) mM/mL (▲), 3.47 (or 1.25) mM/mL (○), 1.25 (or 0.45) mM/mL (●), 0.625 (or 0.225) mM/mL (□), and 0.104 (or 0.0375) mM/mL (■); the corresponding sample loads [or the reduced values (to $\phi = 1$ cm)] are 0.08 (or 0.22), 0.15 (or 0.42), 0.25 (or 0.69), 0.35 (or 0.97), and 0.85 (or 2.4) mg, respectively. The total column length, L, applied to the experiments are 0.5, 1, 3, 13 (= 3 + 10), 33

(B) DNA

The points in Fig. 4(c) are experimental plots of $m_{elu(P)}$ for DNA chromatographic peak versus L for two different $g'_{(P)}$ [or $g'_{(P)}$ (ϕ = 1 cm)] values: 3.47 (or 1.25) mM/mL and 0.625 (or 0.225) mM/mL; sample load is always within the range of 5–8 μg, which is small enough for m_{elu} to be virtually independent of sample load. For comparison, the corresponding plots for lysozyme and T_2 phage are illustrated in Figs. 4(a) and 4(e), respectively (for T_2 phage, see the Discussion Section). It can be seen that, with DNA, m_{elu} depends less and more strongly upon both L and $g'_{(P)}$ (Fig. 4c) than with lysozyme (Fig. 4a) and T_2 phage (Fig. 4e), respectively. The continuous curves in Fig. 4(c) are theoretical, calculated by using Eq. (5) in the Appendix (see Discussion Subsection B).

The points in Fig. 4(d) are experimental plots of $m_{elu(P)}$ versus ln $s_{app(P)}$ where the same experimental data as used in Fig. 4(c) are applied. It can be seen that, with DNA, m_{elu} increases more and less slowly with an increase of $s_{app(P)}$ (Fig. 4d) than with lysozyme (Fig. 4b) and T_2 phage (Fig. 4f), respectively. The continuous straight line in Fig. 4(d) represents both the regression line of $m_{elu(P)}$ on ln $s_{app(P)}$ and the theoretical curve (being virtually a straight line) calculated by using Eq. (5) in the Appendix (see Discussion Subsection B).

In Fig. 4(g), B' for DNA is illustrated as a function of $m_{(P)}$ which has been calculated by using Eq. (3) in the Appendix (cf. the legend of Fig. 4g and Discussion Subsection B). It can be seen in Fig. 4(g) that the transition of B' from $\approx$0 to 1 with an increase of m with DNA occurs more and less rapidly than those with lysozyme and T_2 phage, respectively.

Since the DNA sample is heterogeneous, giving a chromatographic peak with a large width (cf. the explanation of $m_{elu(P)}$ in Important Experimental Parameters), the behavior of $\sigma_{(P)}$ or $\sigma_{(K^+)}$ for DNA was not pursued.

(= 3 + 30), 93 (= 3 + 3 × 30), 156 (= 2 × 3 + 5 × 30), and 216 (= 2 × 3 + 7 × 30) cm. Other experimental conditions are: $m_{in(P)}$ = 1 mM, flow rate = 1.5 mL/min [reduced value (to ϕ = 1 cm) = 4.17 mL/min], P = 0.3–5.0 MPa, T = 15.6–22.6°C. Curves in (a): theoretical curves calculated by using Eq. (5) in the Appendix, where x' = 6, ln q_{app} = 6.74, $\varphi'_{(K^+)}$ = 14 M^{-1}, and $m_{in(K^+)}$ = 1.5 mM. The x', ln q_{app}, and $\varphi'_{(K^+)}$ values are best values estimated from Fig. 4(b). (For details, see Discussion Subsection B). Continuous curves in (b): theoretical curves calculated by using Eq. (6) in the Appendix, where $m_{in(K^+)}$ = 1.5 mM and it has been assumed: x' = 6, ln q = 7.06, and $\varphi'_{(K^+)}$ = 14 M^{-1}. It has also been assumed: θ_0 = 0.020, 0.028, 0.04, 0.05, and 0.1 cm for each curve (from the upper to the lower one). Dotted curves in (b): theoretical curves also calculated by using Eq. (6) in the Appendix under the same assumptions as for the continuous curves except for the θ_0 value; a common value, 0.028 cm, has been assumed for θ_0 associated with any g'. (For details, see Discussion Subsection B).

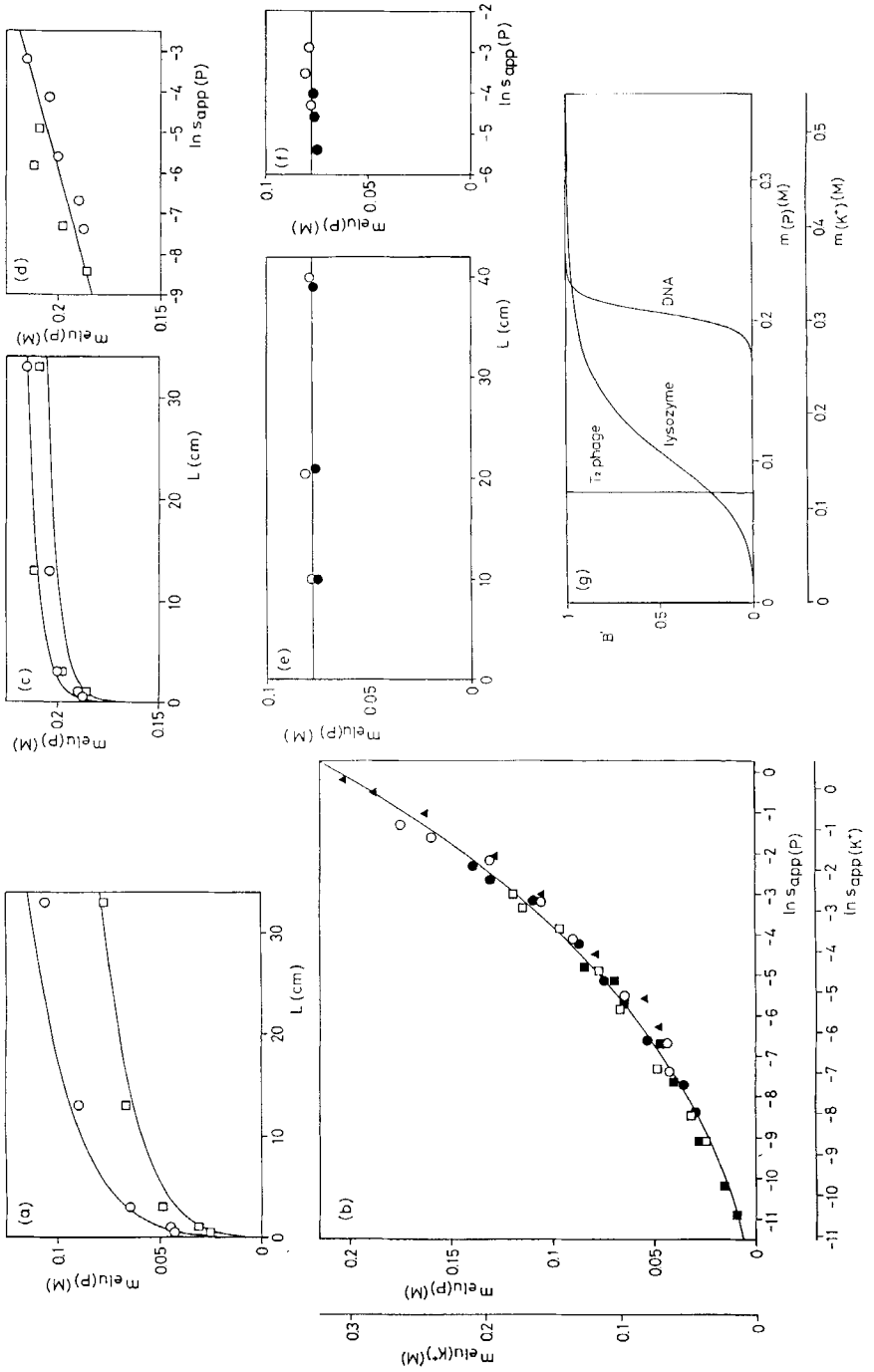

FIG. 4. (a) Points: picked up plots of Fig. 3(a) for lysozyme for two different $g'_{(P)}$ [or $g'_{(P)}(\phi = 1\ \text{cm})$] values: 3.47 (or 1.25) mM/mL (○) and 0.625 (or 0.225) mM/mL (□), where P = 0.3–1.4 MPa and T = 19.5–21.9°C. Curves: theoretical curves (see the legend of Fig. 3a). (b) Points: experimental plots of $m_{elu(P)}$ or $m_{elu(K^+)}$ for lysozyme versus ln $s_{app(P)}$ or ln $s_{app(K^+)}$ where the same data as used in Fig. 3(a) have been used. Curve: theoretical curve giving a best fit with the experimental plots; this has been calculated by using Eq. (5) in the Appendix, where $m_{in(K^+)}$ = 1.5 mM and it has been assumed: x' = 6, ln q_{app} = 6.74, and $\varphi'_{(K^+)} = 14\ M^{-1}$. (For details, see Discussion Subsection B). (c) Points: experimental plots of $m_{elu(P)}$ for DNA versus L for two different $g'_{(P)}$ [or $g'_{(P)}(\phi = 1\ \text{cm})$] values: 3.47 (or 1.25) mM/mL (○) and 0.625 (or 0.225) mM/mL (□); the sample load is always within the range of 5–8 μg. The total column length, L, applied in the experiments are 0.5, 1, 3, 13 (= 3 + 10), and 33 (= 3 + 30) cm. Other experimental conditions are: $m_{in(P)}$ = 0.15 M, flow rate = 0.80 mL/min [reduced value (to ϕ = 1 cm) = 2.22 mL/min], P = 0.1–0.5 MPa, T = 20.5–29.5°C. When L = 13 cm, the m_{elu} value for the experimental points for $g'_{(P)}$ = 3.47 mM/mL is smaller than that for $g'_{(P)}$ = 0.625 mM/mL, which is opposite to the theoretical prediction. This is presumably due to the experimental error. Curves: theoretical curves calculated by using Eq. (5) in the Appendix, where $m_{in(P)}$ = 0.15 M and it is assumed: x' = 72, ln q_{app} = 50.58, and $\varphi'_{(P)} = 5\ M^{-1}$, or x' = 54, ln q_{app} = 60.00, and $\varphi'_{(P)} = 10\ M^{-1}$. Virtually the identical curves can be obtained under either assumption. (For details, see Discussion Subsection B.) (d) Points: experimental plots of $m_{elu(P)}$ for DNA versus ln $s_{app(P)}$ where the same data as used in (c) have been used. Straight line: regression line for $m_{elu(P)}$ on ln $s_{app(P)}$ for the experimental points, on which two theoretical curves (being virtually straight lines) are superimposed. These have been calculated by using Eq. (5) in the Appendix, where $m_{in(P)}$ = 0.15 M and it is assumed: x' = 72, ln q_{app} = 50.58, and $\varphi'_{(P)} = 5\ M^{-1}$, or x' = 54, ln q_{app} = 60.00, and $\varphi'_{(P)} = 10\ M^{-1}$. (For details, see Discussion Subsection B.) (e) Points: experimental plots of m_{elu} for T_2 phage versus L for two different $g'_{(P)}$ [or $g'_{(P)}(\phi = 1\ \text{cm})$] values: ≈ 3.47 (or ≈ 1.25) mM/mL (○) and ≈ 1.25 (or ≈ 0.45) mM/mL (●), obtained for open columns (reproduced from Ref. *6*). Horizontal straight line: theoretical curve (for details, see text). (f) Points: experimental plots of $m_{elu(P)}$ for T_2 phage versus ln $s_{app(P)}$ where the same data as used in (e) have been used. Horizontal straight line: theoretical curve (for details, see text). (g) B' for lysozyme, DNA, and T_2 phage as functions of $m_{(P)}$ or $m_{(K^+)}$, calculated by using Eq. (3) in the Appendix. It is assumed for the lysozyme curve: x' = 6, ln q = 7.06, and $\varphi'_{(K^+)} = 14\ M^{-1}$; for the DNA curve: x' = 72, ln q = 50.90, and $\varphi'_{(P)} = 5\ M^{-1}$, or x' = 54, ln q = 60.32, and $\varphi'_{(P)} = 10\ M^{-1}$. (Virtually the identical curves can be obtained under either assumption.). For the T_2 phage curve, $x' = \infty$. (For details, see Discussion Subsection B.)

DISCUSSION

(A) General Discussion

With lysozyme, the dependence of m_{elu} upon both L and g' (Figs. 3a and 4a), the dependence of m_{elu} upon s_{app} (Fig. 4b) or s (see Eq. 7 in the Appendix), and the dependence of σ upon both L and g' (Fig. 3b) are all parallel with the case of open HA columns (*6–8*) in which plate-like HA crystals similar to those used in the present work are packed. The fact that, with DNA with high molecular masses of 10–50 MDa, m_{elu} depends less strongly upon L, g' and s_{app} (or s) (Figs. 4c and 4d) than with lysozyme with a low molecular mass of 14 kDa (Figs. 4a and 4b) is also parallel with the case of open HA columns (*6–8*). This phenomenon is basically related to the fact that the transition of B' from ≈ 0 to 1 with an increase of m becomes sharper with an increase in the molecular size (Fig. 4g; also see below, and cf. Refs. *9* and *13*).

Figures 4(e) and 4(f) illustrate both the experimental plots and the theoretical curves for T_2 phage which correspond to those shown in Figs. 4(a)–(d). The experimental plots in Fig. 4(e) have been reproduced from Fig. 1(E) in an earlier paper (*6*) obtained for open columns. A T_2 phage particle is constituted of a prolated icosahedral head of 650 × 950 Å and a tail of 250 × 1100 Å, the former containing a DNA with a molecular mass of 100 MDa [14]. It can be seen in Figs. 4(e) and 4(f) that m_{elu} for T_2 phage is virtually independent of both L and g' or of s_{app}. In Fig. 4(g), B' for T_2 phage is plotted as a function of m, where it can be seen that the transition of B' with an increase of m occurs stepwise (for details, see Subsection B).

Figure 3(b) shows (in parallel with the case of open columns; Fig. 1 of Ref. *8*) that, for a given slope, g', of the molarity gradient, a column length, L^*, exists that minimizes the width, σ, of the lysozyme chromatographic peak (see Results Subsection A). On the other hand, by using open columns it was shown (*6, 8*) that the dependences of both m_{elu} and σ upon L for molecules with similar sizes are parallel to one another; this means that the L^* value estimated for lysozyme (Fig. 3b) is common (from a practical point of view) to any molecules with molecular masses of the order of 10 kDa, realizing the optimal separation condition of the molecules provided the slope, g', of the molarity gradient is given. Figure 3(b) also shows that L^* increases and the corresponding σ decreases when g' decreases. This means that the chromatographic efficiency for a mixture of molecules with molecular masses of the order of 10 kDa increases when g' decreases and when L increases appropriately at the same time.

In earlier papers (*1*, *2*) a number of proteins and a *t*-RNA with molecular masses of the order of 10 kDa were chromatographed on plate-like HA packed HPLC columns under three different experimental conditions: (a) $g'_{(P)}$ = 3.47 m*M*/mL [or $g'_{(P)}$ (ϕ = 1 cm) = 1.25 m*M*/mL] and L = 13 cm, (b) $g'_{(P)}$ = 0.625 m*M*/mL [or $g'_{(P)}$ (ϕ = 1 cm) = 0.225 m*M*/mL] and L = 33 cm, and (c) $g'_{(P)}$ = 0.104 m*M*/mL [or $g'_{(P)}$ (ϕ = 1 cm) = 0.0375 m*M*/mL] and L = 213 or 216 cm. Figure 3(b) shows that the L values associated with the corresponding $g'_{(P)}$ in Refs. *1* and *2* are all optimal from the practical point of view. The experiments in Refs. *1* and *2* demonstrate that the chromatographic efficiency increases, in fact, in the order of the experimental condition (a), (b), and (c) in accordance with the prediction from Fig. 3(b). (See Figs. 4–6 and 8–10 of Ref. *1* and Figs. 1 and 4–6 of Ref. *2*.)

The transition of B' from $\approx$0 to 1 with an increase of m becomes sharper when the molecular size increases (Fig. 4g), and m_{elu} becomes less dependent upon s_{app} (i.e., upon both g' and L) with an increase in the molecular size (Figs. 4a–4f). The fact that the L^* value associated with the given g' decreases with an increase in the molecular size can qualitatively be understood if the case with an extremely large molecular size (like that with T_2 phage) is considered. Thus, since, in this instance, the transition of B' from $\approx$0 to 1 occurs virtually stepwise, let m° be the m value at which the step transition of B' occurs. Under this situation the buffer A molarity gradient would simply pass the initial band of the molecules adsorbed at the inlet of the column until the molarity, m, at the column inlet reaches the critical molarity m° (since $B' = 0$ when $m < m^\circ$). When m reaches m° at the column inlet, the desorption of the molecules would occur suddenly, and the molecular band would begin to migrate toward the outlet of the column with a velocity equal to the migration velocity of the molarity gradient (since $B' = 1$ when $m > m^\circ$). During the migration of the molecules on the column, the width of the molecular band would continue to increase by diffusion since all the molecules exist in the mobilie phase ($B' = 1$); the center of the molecular band would always be situated at the critical molarity m° of the gradient. This means, first, that the elution molarity m_{elu} is always equal to m° independently of s_{app}, i.e., both g' and L. (This is experimentally demonstrated for T_2 phage in both Figs. 3e and 3f.) Second, L^* is infinitesimal, i.e., the shorter the total column length, the smaller is the width, σ, of the chromatographic peak. Quantitative arguments concerning how the optimal column length L^* changes when the sample molecular size changes are made in the earlier papers (*6*, *8*, *10*). With respect to molecules with molecular masses larger than the order of 10 kDa, it is difficult to obtain the ideal experimental plots of σ versus L as shown in Fig. 3(b) for lysozyme with a molecular

mass of 14 kDa; this is because almost all molecules with high molecular masses are found to be heterogeneous in some manner.

Earlier, high chromatographic efficiencies were attained for proteins with molecular masses of 300–500 kDa (collagen and myosin) by using the L of 13 cm (instead of 33 cm) when $g'_{(P)} = 0.625$ mM/mL [or $g'_{(P)}$ (ϕ = 1 cm) = 0.225 mM/mL] (see Figs. 12 and 14 of Ref. *1*); with DNA with molecular masses of 10–50 MDa, the L of 36 cm (instead of 213 or 216 cm) was applied when $g'_{(P)} = 0.104$ mM/mL [or $g'_{(P)}$ (ϕ = 1 cm) = 0.0375 mM/mL] (see Fig. 2 of Ref. *2*).

(B) Relationship with the Chromatographic Theory (cf. Appendix)

Equation (5) in the Appendix predicts that the elution molarity, m_{elu} or μ, of a chromatographic peak be determined by the parameter s, the product of g' and L', or g and L. Therefore, if our theory is correct, the five arrangements of the experimental points in Fig. 3(a) should converge into a single arrangement when m_{elu} is plotted versus s or s_{app} instead of L; s_{app} is 1/0.726 times as large as s (see Eq. 7 in the Appendix). The points in Fig. 4(b) are experimental plots of m_{elu} versus ln s_{app}. Figure 4(b) demonstrates that the five arrangements of the experimental points in Fig. 3(a), in fact, converge into a single arrangement, confirming the correctness of the theory.

The curve in Fig. 4(b) is theoretical calculated by using Eq. (5) in the Appendix; a best fit with the experiment has been obtained by assuming $x' = 6$, ln $q_{app} = 6.74$, and $\varphi'_{(K^+)} = 14\ M^{-1}$ and by using the value, 1.5 mM, for $m_{in(K^+)}$, where both $\varphi'_{(K^+)}$ and $m_{in(K^+)}$ are concerned with potassium ions in buffer A since lysozyme is adsorbed onto P sites on the c crystal surface and it competes with potassium ions from the buffer for adsorption (see Ref. *1*). Good fits with the experiment are available between two combinations of the experimental parameters: ($x' = 5$, ln $q_{app} = 6.84$, $\varphi'_{(K^+)} = 20\ M^{-1}$) and ($x' = 7$, ln $q_{app} = 6.39$, $\varphi'_{(K^+)} = 10\ M^{-1}$). It should be noted that, in Eq. (5), the parameters q and s are involved in the form of the product $q \cdot s$. Therefore, by using the parameter q_{app} (instead of q), μ can be represented as a function of s_{app} (instead of s) (see both Eqs. 7 and 8 in the Appendix); ln q can be calculated from ln q_{app} by using Eq. (8) in the Appendix. Thus, a best ln q value can be estimated to be 7.06, inserted between two limiting values of 7.16 and 6.71. [With classical open HA columns, a best fit between theory and experiment was obtained when $x' = 7$, ln $q = 6.7$, and $\varphi'_{(K^+)} = 9\ M^{-1}$ (*8*). These values are nearly or almost equal to those obtained above for HPLC.]

It should be noted that the coincidence of the theoretical curve with the

experimental plot (Fig. 4b) is excellent, explaining a slight displacement from the linearity of the arrangement of the experimental points. It should also be noted that the value, 6 ± 1, of x' estimated above is very reasonable from Fig. 5 where a lysozyme molecule adsorbed on P sites on the **c** crystal surface of HA is schematically illustrated (for details, see the legend of Fig. 5). It can be deduced from Fig. 5 that a lysozyme molecule effectively covers several P sites, explaining the x' value of 6 ± 1 (for the precise meaning of "covering," see the Appendix).

The curves in both Figs. 3(a) and 4(a) are theoretical, calculated by using Eq. (5) in the Appendix, where $x' = 6$, $\ln q_{app} = 6.74$, $\varphi'_{(K^+)} = 14\ M^{-1}$, and $m_{in(K^+)} = 1.5$ mM. The x', $\ln q_{app}$ and $\varphi'_{(K^+)}$ values are best values estimated from Fig. 4(b).

The continuous curves in Fig. 3(b) are theoretical, calculated by using Eq. (6) in the Appendix, where $x' = 6$, $\ln q = 7.06$, $\varphi'_{(K^+)} = 14\ M^{-1}$, and $m_{in(K^+)} = 1.5$ mM. Since, in Eq. (6), the parameters q and s do not always appear in the form of the product $q \cdot s$, it is necessary to recalculate q from q_{app} by using Eq. (8) in the Appendix. For the calculation of the theoretical curves it has been assumed that $\Theta_0 = 0.020$, 0.028, 0.04, 0.05, and 0.1 cm for the curves from the upper to the lower one in order to have best fits with experiment. (The theoretical curve becomes less sensible to the fluctuation in the Θ_0 value as g' decreases. This is the reason why Θ_0 for $g'_{(P)} \geqslant 3.47$ mM/mL has been represented by using two significant figures in contrast to Θ_0 for $g'_{(P)} \leqslant 1.25$ mM/mL which has been represented by using only one significant figure.) It can be seen in Fig. 3(b) that the theory explains very well the fact that σ, in general, decreases

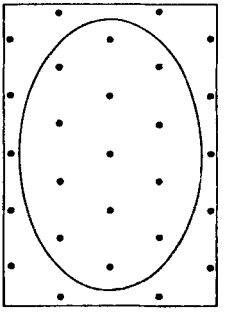

FIG. 5. Schematic representation of a lysozyme molecule adsorbed on P sites on the **c** crystal surface of HA; it has been assumed that lysozyme is approximately represented by a prolate spheroid of dimensions $4.5 \times 3 \times 3$ nm. P sites are arranged hexagonally on the **c** crystal surface with a minimal interdistance of 942 pm [1]. (Reproduced from Ref. 7.)

very rapidly with an increase of L when L is small, but that σ increases slowly after the first rapid decrease.

The dotted curves in Fig. 3(b) are also theoretical, calculated by using Eq. (6) in the Appendix under assumptions of $x' = 6$, $\ln q = 7.06$, $\varphi'_{(K^+)} = 14\ M^{-1}$, and $m_{in(K^+)} = 1.5$ mM. A common value, 0.028 cm, has been assumed for Θ_0 associated with any g', however.

Equation (6) in the Appendix has been derived for quasi-static chromatography (*11*). In this ideal chromatography, Θ_0 should be constant, independent of g'. It can be seen in Fig. 3(b), however, that the coincidence between theory and experiment occurs only approximately if a constant Θ_0 value is assumed (dotted curves in Fig. 3b); it is only by increasing the Θ_0 value with a decrease of g' that a good coincidence can be obtained (continuous curves in Fig. 3b). This is presumably due to the fact that, in the actual chromatography, the quasi-static condition (Appendix I of Ref. *11*) is realized only approximately.

Figure 1 of an earlier paper (*8*) illustrated the corresponding (L, σ) experimental plots and the theoretical curves calculated by using a constant Θ_0 value for classical open HA columns, where a good fit between theory and experiment can be seen despite the fact that Θ_0 is constant (although the experimental plots in Ref. *8* are much more fluctuating than the plots in Fig. 3b). The good fits presumably arises from the fact that the best constant Θ_0 value, 0.3 cm, obtained for open columns is about 10 times as large as the corresponding value, 0.028 cm, estimated from Fig. 3(b) for HPLC. It can be deduced that, with classical open columns, the effect (as reflecting upon the Θ_0 value) of longitudinal molecular diffusion that arises from the first type of flow heterogeneity in the column (see Appendix I of Ref. *11*) is about 10 times as large as the same effect with HPLC columns; therefore, the effect of the other kinds of longitudinal molecular diffusion in the classical column is virtually hidden within the former effect, thus realizing almost ideally the condition of quasi-static chromatography (see Appendix I of Ref. *11*).

The curve increasing most slowly with an increase of $m_{(P)}$ or $m_{(K^+)}$ in Fig. 4(g) represents B' for lysozyme as a function of $m_{(K^+)}$; this has been calculated by using Eq. (3) in the Appendix in which $x' = 6$, $\ln q = 7.06$, and $\varphi'_{(K^+)} = 14\ M^{-1}$.

The straight line in Fig. 4(d) is the regression line for $m_{elu(P)}$ on $\ln s_{app(P)}$ for the experimental plots of DNA in the same figure; DNA is adsorbed onto C sites on the **a** or **b** crystal surface, and it competes with phosphate ions from the buffer A for adsorption (see the earlier paper, Ref. *1*). It was mentioned above that the value $9\ M^{-1}$ of $\varphi'_{(K^+)}$ estimated for classical open HA columns is in the vicinity of the values $10\text{–}20\ M^{-1}$ estimated from Fig. 4(b) for HPLC. Earlier (*15*), the $\varphi'_{(P)}$ value for classical columns was

estimated to be 4.6–6.7 M^{-1}. We, therefore, simply assume that the $\varphi'_{(P)}$ value for HPLC is 5–10 M^{-1}. When $\varphi'_{(P)} = 5\ M^{-1}$, assuming $x' = 72$ and ln $q_{app} = 50.58$ (or ln $q = 50.90$; cf. Eq. *8* in the Appendix), then a curve (being virtually a straight line) that coincides with the regression line in Fig. 4(d) can be calculated by using Eq. (5) in the Appendix, where $m_{in(P)} = 0.15\ M$. When $\varphi'_{(P)} = 10\ M^{-1}$, the identical curve (or the straight line) can be obtained by assuming $x' = 54$ and ln $q_{app} = 60.00$ or ln $q = 60.32$).*

Taking into account the geometrical arrangement of adsorbing sites on the crystal surface and the fact that the molecular masses of the DNA sample used in Fig. 4(d) are 10–50 MDa [700–3500 times as large as the molecular mass of lysozyme (14 kDa); see Materials and Methods], the x' value, 54–72, estimated above (only 8–14 times as large as the x' value, 5–7, for lysozyme) seems to be much too small if the molecule is adsorbed on the crystal surface by using the total molecular structure or a considerable part of it. It can be deduced that the double-stranded DNA molecule takes a conformation close to a random coil in solution, and that the molecule is adsorbed on the HA surface by using only a small part of the total structure, conserving the random coil conformation in solution. In an earlier paper (*16*) the same conclusion was reached from a different point of view by analyzing the chromatographic data obtained by Wilson and Thomas (*17*).

The curves in Fig. 4(c) are theoretical, calculated by using Eq. (5) in the Appendix where $m_{in(P)} = 0.15\ M$, and it is assumed that $x' = 72$, ln $q_{app} = 50.58$, and $\varphi'_{(P)} = 5\ M^{-1}$, or $x' = 54$, ln $q_{app} = 60.00$, and $\varphi'_{(P)} = 10\ M^{-1}$. Virtually identical curves can be obtained under either assumption.

In Fig. 4(g), B' for DNA is plotted as a function of m; this has been calculated by using Eq. (3) in the Appendix where it is assumed that $x' = 72$, ln $q = 50.90$, and $\varphi'_{(P)} = 5\ M^{-1}$, or $x' = 54$, ln $q = 60.32$, and $\varphi'_{(P)} = 10\ M^{-1}$. Virtually identical curves can be obtained under either assumption.

The horizontal line in Fig. 4(f) represents the theoretical curve for T_2 phage that has simply been deduced from the arrangement of the experimental plots, from which it can be estimated that the x' value is virtually infinity. The horizontal line in Fig. 4(e) is also theoretical, derived from the horizontal line in Fig. 4(f). By using the horizontal line in Fig. 4(e) or that in Fig. 4(f), the function $B'(m)$ for T_2 phage can be calculated; this is illustrated in Fig. 4(g). It can be seen in Fig. 4(g) that B'

*With an increase of x', the theoretical curve, in general, becomes less sensible to the values of the parameters φ' and ln q_{app} (or ln q), and it becomes difficult to evaluate their exact values.

for T_2 phage with $x' = \infty$ shows a step transition from 0 to 1 with an increase of m.

Finally, the dependence of the chromatogram upon sample load as shown in Fig. 1 can also be analyzed on the basis of the chromatographic theory developed in an earlier paper (*18*). However, we do not treat this problem here since the theory is more complicated than that shown in the Appendix and is out of the scope of this paper.

APPENDIX

Let us first specify two points of view on gradient chromatography. These are summarized in Fig. A1, where the abscissa L' represents the general longitudinal column position expressed as the sum of interstitial volumes involved between the column inlet and the column position, L, under consideration. In some instances, L' and L represent the *total* interstitial volumes and the *total* length of the column, respectively. The ordinate m represents the concentration or the molarity of a component (i.e., phosphate or potassium ions) of the carrier liquid that constitutes a linear gradient in the column. The oblique straight line represents the linear molarity gradient with slope g' occurring at time t. The slope g' is defined as positive in order for it to have a dimension of molarity/

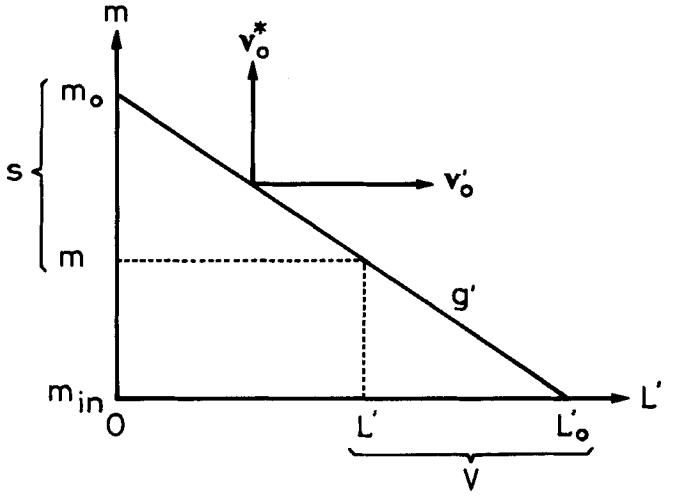

FIG. A1. Schematic representation of two points of view on gradient chromatography. (Reproduced from Ref. *11*.)

volume. L'_0 and m_0 show the column position at which the beginning of the gradient exists and the molarity of the gradient at the inlet of the column, respectively. m_{in} is the initial molarity of the gradient introduced at the inlet ($L' = 0$) of the column at time 0.

In the first point of view, it is the column itself that is fixed. Both the molarity gradient and the band of the sample molecules migrate in the L' direction on the (L', m) plane; v'_0 in Fig. A1 represents the migration velocity (in units of volume/time) of the gradient observed at a given longitudinal position L' on the column. Elution volume V occurring at the position L' can be written as

$$V = L'_0 - L' = (m - m_{in})/g' \tag{1}$$

where both L' and m_{in} are constant, and both L'_0 and m increase with time t, m being defined as the molarity of the gradient at the given column position L' (i.e., the column outlet in many instances). Therefore, V increases with time t. In other words, V is a chromatographic expression of time in the first point of view.

In the second point of view, it is the molarity gradient that is fixed. Both the column and the band of the sample molecules migrate in the m direction on the (L', m) plane. It can be considered that the oblique straight line in Fig. A1 represents the linear "gradient" of column position L' (with slope $1/g'$) rather than the linear molarity gradient (with slope g'); v^*_0 in Fig. A1 represents the migration velocity (in units of molarity/time) of the "gradient" along the molarity gradient. Here, it is possible to find a parameter s (with a dimension of molarity) that corresponds to V in the first point of view, occurring at a given position m on the molarity gradient. This can be written as

$$s = m_0 - m = g'L' \tag{2}$$

where m is constant, and both m_0 and L' increase with time t, L' now being defined as the longitudinal position on the column at which the molarity of the gradient is always equal to m. Therefore, s increases with time t. In other words, s is a chromatographic expression of time in the second point of view.

The gradient chromatography is understandable from the second point of view by considering an abstract flux of molecules occurring *in the mobile phase* in the column (*9, 11*). Especially in the case of small sample loads with quasi-static chromatography when longitudinal molecular diffusion in the column is mostly contributed from the first type of flow heterogeneity in the carrier liquid [for details, see Appendix I of an earlier

paper (*11*)], a simple theoretical expression of the chromatogram can be derived (*11*).

On the other hand, a competitive model was first introduced over 15 years ago for the adsorption and desorption mechanism occurring in the HA column (*13*). The model states that adsorbing sites are arranged in some manner on the surfaces of HA crystals packed in the column; the sample molecules (with adsorption groups) and a gradient element (i.e., phosphate or potassium ions) compete for adsorption onto the sites of the packed HA particles (*11*, *13*). A gradient element covers a single site when it is adsorbed whereas a sample molecule, in general, covers plural sites (*11*, *13*). [In the introductory part of an earlier paper (*1*), the concrete structure and the arrangement of the adsorbing sites on the crystal surface of HA are mentioned, and the adsorption configuration of a macromolecule on the crystal surface is argued.]

On the basis of the competitive model, parameter B' (see Important Experimental Parameters) can be represented (*7*, *9*, *11*, *13*) as

$$B'(m) = \frac{1}{1 + q(\varphi' m + 1)^{-x'}} \tag{3}$$

where q, φ', and x' are positive constants, x' representing the number of adsorbing sites of HA covered by an adsorbed sample molecule, i.e., the number of adsorbing sites of HA on which the adsorption of gradient elements (i.e., competing ions) is impossible due to the presence of an adsorbed sample molecule. [For the physical meanings of q and φ', see an earlier paper (*8*).]

In the case of small sample loads with quasi-static chromatography (see above), by introducing Eq. (3), the theoretical chromatogram, $f_s(m)$, for a molecular component under consideration in the mixture can be represented as

$$f_s(m) = \frac{1}{\sqrt{2\pi}\sigma(s)} e^{-[m-\mu(s)]^2/[2[\sigma(s)]^2]} \tag{4}$$

where

$$\mu(s) = \frac{1}{\varphi'} \{[(x' + 1)\varphi' qs + (\varphi' m_{in} + 1)^{x'+1}]^{1/(x'+1)} - 1\} \tag{5}$$

and

$$\sigma(s) = \sqrt{2\Theta g' s}\{1 + q[\varphi'\mu(s) + 1]^{-x'}\}$$
$$= \sqrt{2\Theta_0 g s}\{1 + q[\varphi'\mu(s) + 1]^{-x'}\} \quad (6)$$

In Eq. (6), g represents the slope of the molarity gradient expressed in units of molarity/length; Θ and Θ_0 are positive constants with dimensions of volume and of length, measuring the longitudinal molecular diffusion in the column, respectively (*9*). Equation (5) is even valid for nonquasi-static chromatography (*11*).

If the sample molecule has a very large molecular size ($x' \gg 1$), $\mu(s)$ (Eq. 5) tends to a constant value of m^0 independent of s; $\sigma(s)$ (Eq. 6) tends to $\sqrt{2\Theta g' s}$ or $\sqrt{2\Theta_0 g s}$ at the same time.

It should be noted that Eq. (4) involves the parameter s, which represents time in the second point of view. In the spontaneous first point of view, s represents the product of g' and L' (Eq. 2), or the product of g and L, where L' or L represents the *total* length of the column.

In the plots of Figs. 4(b), 4(d), and 4(f), however, the parameter s_{app} is used instead of s, where s_{app} represents the product of g' (ϕ = 1 cm) and L. Since the ratio of the volume occupied by HA crystals to the total packed crystal volume in the column is estimated to be 0.075 (Materials and Methods), then by representing length and volume in units of centimeters and milliliters, respectively, s can be written in terms of s_{app} as

$$s = \frac{\pi}{4}(1 - 0.075)s_{app} = 0.726 s_{app} \quad (7)$$

Finally, from Figs. 4(b) and 4(d), the apparent parameters $\ln q_{app}$ for lysozyme and DNA can be directly evaluated instead of $\ln q$, respectively, where q and q_{app} are related by the relationship

$$q = q_{app}/0.726 \quad (8)$$

Acknowledgments

The authors thank Mr K. Ikeda and Mr W. Kobayashi for carrying out some experiments.

REFERENCES

1. T. Kawasaki, S. Takahashi, and K. Ikeda, *Eur. J. Biochem., 152,* 361 (1985).
2. T. Kawasaki, K. Ikeda, S. Takahashi, and Y. Kuboki, *Ibid., 155,* 249 (1986).

3. T. Kawasaki, W. Kobayashi, K. Ikeda, S. Takahashi, and H. Monma, *Ibid., 157,* 291 (1986).
4. T. Kawasaki, M. Niikura, S. Takahashi, and W. Kobayashi, *Biochem. Int., 13,* 969 (1986).
5. T. Kawasaki and W. Kobayashi, *Ibid., 14,* 55 (1987).
6. T. Kawasaki and G. Bernardi, *Biopolymers, 9,* 257 (1970).
7. T. Kawasaki, *J. Chromatogr., 93,* 313 (1974).
8. T. Kawasaki, *Sep. Sci. Technol., 16,* 439 (1981).
9. T. Kawasaki, *Ibid., 16,* 817 (1981).
10. T. Kawasaki, *Ibid., 16,* 885 (1981).
11. T. Kawasaki, *Ibid., 22,* 121 (1987).
12. G. Cuny, P. Soriano, G. Macaya, and G. Bernardi, *Eur. J. Biochem., 115,* 227 (1981).
13. T. Kawasaki, *Biopolymers, 9,* 277 (1970).
14. S. E. Luria and J. E. Darnell Jr., *General Virology,* 2nd ed., Wiley, New York, 1967, p. 187.
15. T. Kawasaki, *J. Chromatogr., 151,* 95 (1978).
16. T. Kawasaki, *Sep. Sci. Technol., 17,* 785 (1982).
17. D. A. Wilson and C. A. Thomas Jr., *Biochim. Biophys. Acta, 331,* 333 (1973).
18. T. Kawasaki, *Sep. Sci. Technol., 17,* 1397 (1982).

Received by editor December 10, 1986
Revised March 30, 1987